

# PARALLEL MULTILEVEL METHODS FOR SOLVING THE Darcy–FORCHHEIMER MODEL BASED ON A NEARLY SEMICOERCIVE FORMULATION\*

JONGHO PARK<sup>†</sup> AND S. MAJID HASSANIZADEH<sup>‡</sup>

**Abstract.** High-velocity fluid flow through porous media is modeled by prescribing a nonlinear relationship between the flow rate and the pressure gradient, called Darcy–Forchheimer equation. This paper is concerned with the analysis of parallel multilevel methods for solving the Darcy–Forchheimer model. We begin by reformulating the Darcy–Forchheimer model as a nearly semicoercive convex optimization problem via the augmented Lagrangian method. Building on this formulation, we develop a parallel multilevel method within the framework of subspace correction for nearly semicoercive convex problems. The proposed method exhibits robustness with respect to both the nearly semicoercive nature of the problem and the size of the discretized system. To further enhance convergence, we incorporate a backtracking line search scheme. Numerical results validate the theoretical findings and demonstrate the effectiveness and superiority of the proposed approach.

**Key words.** Darcy–Forchheimer model, Multilevel methods, Subspace correction methods, Nearly semicoercive problems, augmented Lagrangian method

**AMS subject classifications.** 65N55, 65N20, 76S05, 90C25

**1. Introduction.** The Darcy–Forchheimer model characterizes a nonlinear relationship between flow rate and pressure gradient in porous media, and arises in a variety of important applications (see, e.g., [49]). A common situation relates to groundwater flow in high-permeability zones, such as karstic aquifers (see [36]). Also, the flow velocity is high around wellbores in oil and gas reservoirs, in geothermal reservoirs, or in CO<sub>2</sub> sequestration systems, where fluids are extracted or injected (cf. [12]). Another example is in gas reservoirs where high compressibility and velocity make inertial effects important [38, 52]. In some groundwater contamination systems, such as reactive barriers and funnel and gate systems, high groundwater velocity is encountered [16]. Finally, in some manufactured porous media, such as porous catalysts or packed columns, high-speed gas or liquid flows lead to non-Darcy behavior [22, 55]. Various studies have shown that using standard groundwater models, which are based on Darcy models, fail to predict flow fields in systems described above. Often they underestimate velocity by orders of magnitude for a given pressure distribution; see e.g., [26].

Due to its significance, substantial research has been dedicated to developing numerical methods for the Darcy–Forchheimer model. Regarding numerical discretizations, many studies have focused on finite element approaches, which are often classified based on the choice of weak formulation. In [40, 41], mixed finite element methods were developed using a weak formulation with the primal space  $H(\operatorname{div}; \Omega) \cap L^3(\Omega)^d$  and the dual space  $L^2(\Omega)$ , where  $d$  denotes the spatial dimension of the domain  $\Omega$ . In contrast, studies such as [17, 34, 48] adopted a weak formulation with the primal space  $L^3(\Omega)^d$  and the dual space  $W^{1, \frac{3}{2}}(\Omega)$ . For the corresponding discretization,

---

\*This work was conducted while the second author was a visiting professor at KAUST, hosted by the Computer, Electrical and Mathematical Sciences and Engineering Division.

<sup>†</sup>Applied Mathematics and Computational Sciences Program, Computer, Electrical and Mathematical Sciences and Engineering Division, King Abdullah University of Science and Technology (KAUST), Thuwal 23955, Saudi Arabia ([jongho.park@kaust.edu.sa](mailto:jongho.park@kaust.edu.sa)).

<sup>‡</sup>Stuttgart Center for Simulation Science (SimTech), Integrated Research Training Group SFB 1313, Stuttgart University, Germany; Department of Earth Sciences, Utrecht University, 3584, CB, Utrecht, the Netherlands ([S.M.Hassanizadeh@uu.nl](mailto:S.M.Hassanizadeh@uu.nl)).

several numerical solvers have been proposed. A Peaceman–Rachford-type iterative method was proposed in [18], while a nonlinear multigrid method for the coupled nonlinear system was developed in [23]. Furthermore, a monolithic multigrid method for coupled problems on fractured domains was introduced in [3]. In [15], a two-level discretization based on a mixed formulation was investigated to reduce the computational cost associated with the nonlinear component. More recently, transformed primal-dual methods with variable preconditioners were studied in [10].

The aim of this paper is to develop efficient numerical methods for the Darcy–Forchheimer model. Following the multilevel approach adopted in [3, 23], we build on the well-established philosophy of leveraging hierarchical solvers for the nonlinear systems. Multilevel methods are among the most powerful tools in the design of numerical solvers for scientific computing and have been extensively studied. Representative works include [7, 14, 53, 54], where rigorous convergence theories for multilevel methods were developed. Multilevel methods have also been successfully applied to linear problems involving vector fields; see, e.g., [2, 21]. In addition to the aforementioned studies [3, 23], multilevel techniques have been successfully applied to a wide range of nonlinear problems. The design and analysis of multilevel methods for nonlinear problems remain active areas of research (see, e.g., [9]).

Although the multilevel methods for the Darcy–Forchheimer model have demonstrated excellent numerical performance in practice, a rigorous theoretical foundation has remained elusive due to the complexity of the coupled nonlinear system.

In this paper, we propose multilevel methods for the Darcy–Forchheimer model whose numerical performance is supported by mathematical analysis. The main idea is to reformulate the Darcy–Forchheimer model to a convex optimization problem using the augmented Lagrangian method [20, 45]. While this strategy was originally proposed for linear problems [31, 32], we extend it here to the nonlinear setting. Once the model is casted into a convex optimization framework, we design parallel multilevel solvers grounded in the theory of subspace correction methods for convex optimization [42, 43, 51], which has been proven effective for broad class of nonlinear partial differential equations [29, 44]. In particular, the resulting convex optimization problem is nearly semicoercive, i.e., it becomes ill-conditioned as the augmented Lagrangian parameter  $\epsilon$  tends to zero. To address this challenge, we adopt the recently proposed framework of subspace correction methods tailored to nearly semicoercive convex optimization problems [30].

The main contributions are as follows:

- We show that the coupled nonlinear Darcy–Forchheimer model can be reformulated as a nearly semicoercive convex optimization problem via the augmented Lagrangian approach.
- Based on this formulation, we design and analyze efficient parallel multilevel methods.

The remainder of this paper is organized as follows. In section 2, we review finite element discretizations for the Darcy–Forchheimer model. In section 3, we present the reformulation of the Darcy–Forchheimer model as a nearly semicoercive convex optimization problem. In section 4, we propose and analyze relevant parallel multilevel methods. In section 5, we report numerical results that demonstrate the performance of the proposed methods. Finally, in section 6, we provide a summary and conclusions.

**2. The Darcy–Forchheimer model.** In this section, we briefly review the mathematical formulation of the Darcy–Forchheimer model and its finite element discretization. Relevant references include [17, 23, 40].

**2.1. The continuous problem.** Let  $\Omega \subset \mathbb{R}^d$  be a bounded polyhedral domain with  $d = 2, 3$ . The steady-state Darcy–Forchheimer model is governed by the following equations. The nonlinear relationship between the Darcy velocity  $\mathbf{u}$  and pressure  $p$  [19] is given by

$$(2.1a) \quad \frac{\mu}{\rho} \mathbf{K}^{-1} \mathbf{u} + \frac{\beta}{\rho} |\mathbf{u}| \mathbf{u} + \nabla p = \mathbf{f} \quad \text{in } \Omega,$$

where  $\mathbf{K}$  is the permeability tensor,  $\rho$  is the fluid density,  $\mu$  is the fluid viscosity,  $\beta$  is the Forchheimer coefficient, and  $\mathbf{f}$  is the external body force per unit volume.

The conservation of mass is expressed as

$$(2.1b) \quad \operatorname{div} \mathbf{u} = g \quad \text{in } \Omega,$$

where  $g$  is a prescribed source or sink term representing mass production or depletion.

For the boundary condition, for clarity and simplicity, we consider the case of a pure homogeneous Dirichlet boundary condition:

$$(2.1c) \quad p = 0 \quad \text{on } \partial\Omega.$$

**2.2. Finite element approximations.** Various finite element approximations have been proposed in the literature for approximating the Darcy–Forchheimer model [17, 34, 40, 41, 48]; see also [23] and the references therein. Among these, we adopt the approach introduced in [40], which employs Raviart–Thomas-type finite element discretizations [5].

We define the function spaces

$$\begin{aligned} X &= \{ \mathbf{v} \in L^3(\Omega)^d : \operatorname{div} \mathbf{v} \in L^2(\Omega) \}, \\ M &= L^2(\Omega). \end{aligned}$$

Observe that  $X$  is the intersection of two Banach spaces,  $H(\operatorname{div}; \Omega)$  and  $L^3(\Omega)^d$ :

$$X = H(\operatorname{div}; \Omega) \cap L^3(\Omega)^d.$$

Equipped with the norm

$$\|\mathbf{v}\|_X = \left( \|\operatorname{div} \mathbf{v}\|_{L^2(\Omega)}^2 + \|\mathbf{v}\|_{L^2(\Omega)}^2 + \|\mathbf{v}\|_{L^3(\Omega)}^2 \right)^{1/2},$$

the space  $X$  becomes a uniformly smooth and uniformly convex Banach space (cf. [37]).

The weak formulation of (2.1) defined on  $(X, M)$  is as follows: find  $(\mathbf{u}, p) \in X \times M$  such that

$$(2.2) \quad \begin{aligned} \frac{\mu}{\rho} \int_{\Omega} \mathbf{K}^{-1} \mathbf{u} \cdot \mathbf{v} \, dx + \frac{\beta}{\rho} \int_{\Omega} |\mathbf{u}| \mathbf{u} \cdot \mathbf{v} \, dx - \int_{\Omega} p \operatorname{div} \mathbf{v} \, dx &= \int_{\Omega} \mathbf{f} \cdot \mathbf{v} \, dx \quad \forall \mathbf{v} \in X, \\ \int_{\Omega} q \operatorname{div} \mathbf{u} \, dx &= \int_{\Omega} g q \, dx \quad \forall q \in M. \end{aligned}$$

Let  $\mathcal{T}_h$  be a quasi-uniform partition of  $\Omega$  into finite elements, where  $h$  denotes the characteristic mesh size. Let  $X_h \times M_h \subset X \times M$  be a Raviart–Thomas-type conforming mixed finite element space [5] defined on  $\mathcal{T}_h$ . For example, in two dimensions ( $d = 2$ ), if each element  $T \in \mathcal{T}_h$  is a rectangle, the local spaces  $X_h$  and  $M_h$  on  $T$  are defined as

$$X_h(T) := Q_{k+1,k}(T) \oplus Q_{k,k+1}(T), \quad M_h(T) := Q_{k,k}(T),$$

for  $k \geq 0$ , where  $Q_{k,\ell}(T)$  denotes the set of polynomials on  $T$  of degree at most  $k$  and  $\ell$  in each coordinate direction, respectively. Additional examples of Raviart–Thomas-type conforming mixed finite element spaces can be found in [40, Table 1].

The finite element formulation of (2.2) using the discrete space  $X_h \times M_h$  is given as follows: find  $(\mathbf{u}_h, p_h) \in X_h \times M_h$  such that

$$(2.3) \quad \begin{aligned} \frac{\mu}{\rho} \int_{\Omega} \mathbf{K}^{-1} \mathbf{u}_h \cdot \mathbf{v} \, dx + \frac{\beta}{\rho} \int_{\Omega} |\mathbf{u}_h| \mathbf{u}_h \cdot \mathbf{v} \, dx - \int_{\Omega} p_h \operatorname{div} \mathbf{v} \, dx &= \int_{\Omega} \mathbf{f} \cdot \mathbf{v} \, dx \quad \forall \mathbf{v} \in X_h, \\ \int_{\Omega} q \operatorname{div} \mathbf{u}_h \, dx &= \int_{\Omega} g q \, dx \quad \forall q \in M_h. \end{aligned}$$

Existence and uniqueness results for (2.3) can be found in [40, Theorem 3.5].

We define the functional  $F: X \rightarrow \mathbb{R}$  by

$$(2.4) \quad F(\mathbf{v}) = \frac{\mu}{2\rho} \int_{\Omega} \mathbf{K}^{-1} |\mathbf{v}|^2 \, dx + \frac{\beta}{3\rho} \int_{\Omega} |\mathbf{v}|^3 \, dx - \int_{\Omega} \mathbf{f} \cdot \mathbf{v} \, dx, \quad \mathbf{v} \in X.$$

One readily observes that (2.3) corresponds to the optimality condition of the following saddle-point problem:

$$(2.5) \quad \min_{\mathbf{v} \in X_h} \max_{q \in M_h} \left\{ F(\mathbf{v}) - \int_{\Omega} q(\operatorname{div} \mathbf{v} - g) \, dx \right\}.$$

By invoking Fenchel–Rockafellar duality [24, 46], the saddle-point problem (2.5) is equivalent to a constrained convex optimization problem. Namely, (2.3) can be reformulated as a constrained minimization problem, as summarized in Proposition 2.1.

**PROPOSITION 2.1.** *The function  $\mathbf{u}_h \in X_h$  is a primal solution of (2.3) if and only if it solves the following convex optimization problem with a linear constraint:*

$$(2.6) \quad \min_{\mathbf{v} \in X_h} F(\mathbf{v}) \quad \text{subject to} \quad \operatorname{div} \mathbf{v} = g_h,$$

where the functional  $F$  is defined in (2.4), and  $g_h$  is the  $L^2(\Omega)$ -orthogonal projection of  $g$  onto  $M_h$ .

### 3. Reduction to a nearly semicoercive convex optimization problem.

In this section, we show that the finite element discretization (2.3) can be reduced to a nearly semicoercive convex optimization problem if we proceed similarly as in [32, Section 2.2]. More precisely, we show that an iteration of the augmented Lagrangian method [20, 45] for solving the constrained optimization problem (2.6) is equivalent to a nearly semicoercive convex optimization problem [30], where the convergence rate of the augmented Lagrangian method can be arbitrarily fast.

The augmented Lagrangian method [20, 45] for solving (2.6) is summarized in Algorithm 3.1.

In the linear case, for instance when  $\beta = 0$  in (2.3), it was shown in [32, Lemma 2.1] that the augmented Lagrangian method can achieve arbitrarily fast convergence by choosing  $\epsilon$  sufficiently small; similar results are also found in [27, 28]. In Theorem 3.1, we show that this property remains valid for a nonlinear case. We note that the augmented Lagrangian method in a general abstract setting is analyzed in Appendix A.

**THEOREM 3.1.** *Let  $\{(\mathbf{u}_h^{(n)}, p_h^{(n)})\}$  be the sequence generated by the augmented Lagrangian method presented in Algorithm 3.1. Then, there exists a constant  $\mu > 0$ ,*

**Algorithm 3.1** Augmented Lagrangian method for solving (2.6)

---

Given  $\epsilon > 0$ :  
 Choose  $p_h^{(0)} \in M_h$ .  
**for**  $n = 0, 1, 2, \dots$  **do**  
 $\mathbf{u}_h^{(n+1)} = \arg \min_{\mathbf{v} \in X_h} \left\{ F(\mathbf{v}) - \int_{\Omega} p_h^{(n)} \operatorname{div} \mathbf{v} \, dx + \frac{1}{2\epsilon} \int_{\Omega} (\operatorname{div} \mathbf{v} - g_h)^2 \, dx \right\}$   
 $p_h^{(n+1)} = p_h^{(n)} - \epsilon^{-1} (\operatorname{div} \mathbf{u}_h^{(n+1)} - g_h)$   
**end for**

---

independent of  $\epsilon$ , such that

$$D_F^{\text{sym}}(\mathbf{u}_h^{(n+1)}, \mathbf{u}_h) \leq \frac{\epsilon}{4} \|p_h^{(n)} - p_h\|^2 \leq \frac{\epsilon}{4} \left( \frac{\epsilon}{\mu + \epsilon} \right)^{2n} \|p_h^{(0)} - p_h\|^2, \quad n \geq 0,$$

where the symmetrized Bregman divergence  $D_F^{\text{sym}}$  is defined in (A.5).

*Proof.* Thanks to (A.2), Remark A.3, and Theorem A.4, it suffices to verify that  $F^* \circ \operatorname{div}^*$  is locally strongly convex on  $M_h$ , where  $F^*: X_h \rightarrow \overline{\mathbb{R}}$  is the Legendre–Fenchel conjugate of  $F$  defined in (A.4), and  $\operatorname{div}^*: M_h \rightarrow X_h$  denotes the  $L^2(\Omega)$ -adjoint of  $\operatorname{div}: X_h \rightarrow M_h$ . Since  $F$  is locally smooth on  $X_h$  (see section 4.2), it follows from [18] that  $F^*$  is locally strongly convex. Moreover, because  $\operatorname{div}^*$  is injective, the composition  $F^* \circ \operatorname{div}^*$  inherits local strong convexity. This completes the proof.  $\square$

Theorem 3.1 implies that the convergence rate of the augmented Lagrangian method for solving (2.6) can be made arbitrarily fast by choosing  $\epsilon$  sufficiently small. In other words, the number of iterations required to achieve a prescribed level of accuracy becomes very small as  $\epsilon$  decreases. Relevant numerical results illustrating this behavior will be provided in section 5.

In this sense, the mixed formulation (2.3) can be viewed as being reduced to a convex optimization problem of the form

$$(3.1) \quad \min_{\mathbf{v} \in X_h} \left\{ F^\epsilon(\mathbf{v}; q_h) := \frac{1}{2} \int_{\Omega} (\operatorname{div} \mathbf{v} - g_h)^2 \, dx + \epsilon \left[ F(\mathbf{v}) - \int_{\Omega} q_h \operatorname{div} \mathbf{v} \, dx \right] \right\}$$

for some  $q_h \in M_h$ . When there is no ambiguity, we simply write  $F^\epsilon(\mathbf{v}) = F^\epsilon(\mathbf{v}; q_h)$ . In what follows, it suffices to focus on solving (3.1). We denote the solution of (3.1) by  $\mathbf{u}_h^\epsilon \in X_h$ .

A major difficulty in solving (3.1) numerically is that the problem is nearly semi-coercive [30] (cf. nearly singular in the linear case [32]) due to the nontrivial kernel of  $\operatorname{div}$ . As a result, (3.1) becomes increasingly ill-conditioned as  $\epsilon$  becomes small, causing conventional iterative solvers to converge very slowly.

In the following section, we present the construction of an efficient iterative solver for (3.1) that remains robust with respect to both small  $\epsilon$  and the mesh size  $h$ .

**4. Multilevel methods.** In this section, we propose a multilevel method for solving the nearly semicoercive convex optimization problem (3.1) that is robust with respect to both the augmented Lagrangian parameter  $\epsilon$  and the mesh size  $h$ . Building upon the abstract theory of subspace correction methods for solving nearly semicoercive convex optimization problems developed in [30], we construct a patch-based multilevel method with Schwarz smoothers, similarly as in [2, 31]. We also present a backtracking strategy for line search in the multilevel method [43], which makes the

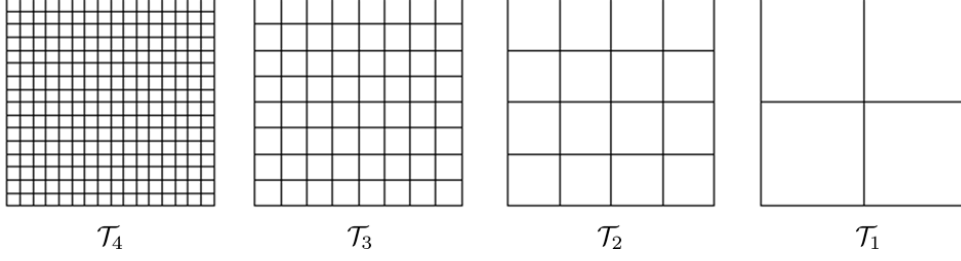


FIG. 1. Multilevel mesh hierarchy  $\{\mathcal{T}_k\}_{k=1}^J$  for a rectangular grid  $\mathcal{T}_h$  ( $J = 4$ ).

algorithm more practical in the sense that it is even faster and does not require a predetermined step size.

**4.1. Multilevel subspace correction.** We assume that the partition  $\mathcal{T}_h$  is part of a nested sequence of quasi-uniform partitions  $\{\mathcal{T}_k\}_{k=1}^J$ , where  $\mathcal{T}_h = \mathcal{T}_J$  and each  $\mathcal{T}_k$ ,  $1 \leq k \leq J$ , has a characteristic element size  $h_k$ . The quasi-uniformity constants are independent of  $k$ , and the mesh sizes satisfy  $h_k \approx \gamma^k$  for some  $\gamma \in (0, 1)$ . See Figure 1 for an example of a rectangular grid  $\mathcal{T}_h$  when  $J = 4$ .

For each  $\mathcal{T}_k$ , we define the finite element space  $V_k$ , of the same type as  $V$ . It follows that

$$V_1 \subset V_2 \subset \cdots \subset V_J = V.$$

Let  $\mathcal{V}_k$  be the set of all internal vertices of  $\mathcal{T}_k$ , and let  $n_k = |\mathcal{V}_k|$ . For each  $x_k^i \in \mathcal{V}_k$ ,  $1 \leq i \leq n_k$ , we define

$$\mathcal{T}_k^i = \{\tau \in \mathcal{T}_k : x_k^i \in \partial\tau\}, \quad \Omega_k^i = \left( \bigcup_{\tau \in \mathcal{T}_k^i} \tau \right)^\circ.$$

We define the subspace  $V_k^i$  as

$$V_k^i = \{v \in V_k : \text{supp } v \subset \overline{\Omega_k^i}\}.$$

Then we have the following vertex-based multilevel space decomposition of  $V$ :

$$(4.1) \quad V = \sum_{k=1}^J \sum_{i=1}^{n_k} V_k^i.$$

Such vertex-based space decomposition for vector field problems was previously considered in, e.g., [2, 31].

Now, we are ready to present our proposed multilevel method. The proposed method is a parallel subspace correction method [30, 42, 51] for solving (3.1) based on the multilevel space decomposition (4.1), as summarized in Algorithm 4.1.

Note that each  $\mathbf{w}_{k,i}^{(n+1)}$ -local problem in Algorithm 4.1 is a convex optimization problem of small dimension, which can be solved robustly and efficiently using second-order optimization algorithms, such as the damped Newton method [6]. Moreover, the for-loops with respect to  $k$  and  $i$  in Algorithm 4.1 can be fully parallelized, making

**Algorithm 4.1** Parallel multilevel method for solving (3.1)

---

Given  $\tau > 0$ :  
 Choose  $\mathbf{u}^{(0)} \in V$ .  
**for**  $n = 0, 1, 2, \dots$  **do**  
   **for**  $k = 1, 2, \dots, J$  **do**  
     **for**  $i = 1, 2, \dots, n_k$  **do**  
        $\mathbf{w}_{k,i}^{(n+1)} = \arg \min_{\mathbf{w}_{k,i} \in V_k^i} F^\epsilon(\mathbf{u}^{(n)} + \mathbf{w}_{k,i})$   
     **end for**  
   **end for**  
    $\mathbf{u}^{(n+1)} = \mathbf{u}^{(n)} + \tau \sum_{k=1}^J \sum_{i=1}^{n_k} \mathbf{w}_{k,i}^{(n+1)}$   
**end for**

---

the algorithm well-suited for implementation on parallel computing architectures. The step size  $\tau$  in Algorithm 4.1 must satisfy a certain condition (to be specified later) to ensure convergence of the algorithm. Nevertheless, as we will show later, the backtracking line search proposed in [43] can be employed to efficiently determine a suitable step size  $\tau$  with only marginal additional computational cost at each iteration of Algorithm 4.1.

*Remark 4.1.* In the linear case, i.e., when  $\beta = 0$  in (3.1), Algorithm 4.1 can serve as a preconditioner. In fact, it coincides with the Bramble–Pasciak–Xu preconditioner [7] or the multilevel additive Schwarz preconditioner [53, 54]. Convergence analysis of multilevel methods for linear problems posed in  $H(\text{div})$  spaces can be found in, e.g., [2, 21].

**4.2. Convergence analysis.** We present a convergence analysis of the proposed multilevel method in Algorithm 4.1, based on the abstract theory developed in [30]. For completeness, a summary of the abstract framework is provided in Appendix B.

Throughout this section, we use the notations  $A \lesssim B$  and  $B \gtrsim A$  to indicate that there exists a positive constant  $C$ , independent of the geometric parameters such as  $h$  and  $J$ , such that  $A \leq CB$ . We write  $A \approx B$  when both  $A \lesssim B$  and  $A \gtrsim B$  hold.

First, we observe that the multilevel space decomposition (4.1) satisfies the strengthened convexity condition (B.3) with

$$(4.2) \quad \tau_0 \gtrsim J^{-1} \approx |\log h|^{-1},$$

as a consequence of a coloring argument [42, Section 5.1] applied at each level.

Let  $F_0$  and  $F_1$  be the semicoercive and coercive parts of the energy functional  $F$ , respectively, namely,

$$(4.3) \quad F_0(\mathbf{v}) = \frac{1}{2} \int_{\Omega} (\text{div } \mathbf{v} - g_h)^2 dx, \quad F_1(\mathbf{v}) = F(\mathbf{v}) - \int_{\Omega} q_h \text{div } \mathbf{v} dx, \quad \mathbf{v} \in V,$$

so that  $F^\epsilon = F_0 + \epsilon F_1$ . We define the Bregman divergences associated with  $F_0$  and  $F_1$  by

$$(4.4) \quad \begin{aligned} d_0(\mathbf{w}; \mathbf{v}) &= F_0(\mathbf{v} + \mathbf{w}) - F_0(\mathbf{v}) - \langle F'_0(\mathbf{v}), \mathbf{w} \rangle, \\ d_1(\mathbf{w}; \mathbf{v}) &= F_1(\mathbf{v} + \mathbf{w}) - F_1(\mathbf{v}) - \langle F'_1(\mathbf{v}), \mathbf{w} \rangle, \end{aligned} \quad \mathbf{v}, \mathbf{w} \in V,$$

where  $\langle \cdot, \cdot \rangle$  denotes the duality pairing on  $V$ . By a direct computation, we observe that

$$(4.5) \quad d_0(\mathbf{w}; \mathbf{v}) = \frac{1}{2} \|\operatorname{div} \mathbf{w}\|_{L^2(\Omega)}^2, \quad \mathbf{v}, \mathbf{w} \in V.$$

Moreover, we have the following lemma concerning  $d_1$ , whose proof is elementary; see, for instance, [13].

LEMMA 4.2. *The Bregman divergence  $d_1$  given in (4.4) satisfies the following:*

- (a)  $d_1(\mathbf{w}; \mathbf{v}) \lesssim \|\mathbf{w}\|_{L^2(\Omega)}^2 + (\|\mathbf{v}\|_{L^3(\Omega)} + \|\mathbf{w}\|_{L^3(\Omega)}) \|\mathbf{w}\|_{L^3(\Omega)}^2$ .
- (b)  $d_1(\mathbf{w}; \mathbf{v}) \gtrsim \|\mathbf{w}\|_{L^2(\Omega)}^2 + \|\mathbf{w}\|_{L^3(\Omega)}^3$ .

In the abstract convergence theory presented in Appendix B, several assumptions are required to ensure the convergence of subspace correction methods; see Theorem B.5 for the convergence result and Assumptions B.1 to B.4 for the corresponding assumptions. In the following, we verify that Algorithm 4.1 satisfies all these assumptions.

The local smoothness condition (Assumption B.1) follows directly from (4.5) and Lemma 4.2(a). The local uniform convexity condition (Assumption B.2) with  $p = 3$  is similarly implied by (4.5) and Lemma 4.2(b). Namely, for any bounded and convex subset  $K \subset V$ , we have

$$(4.6) \quad \mu_{0,K} := \inf_{\mathbf{v}, \mathbf{v}+\mathbf{w} \in K} \frac{d_0(\mathbf{w}; \mathbf{v})}{\|\operatorname{div} \mathbf{w}\|_{L^2(\Omega)}^3} \gtrsim 1, \quad \mu_{1,K} := \inf_{\mathbf{v}, \mathbf{v}+\mathbf{w} \in K} \frac{(d_0 + d_1)(\mathbf{w}; \mathbf{v})}{\|\mathbf{w}\|_X^3} \gtrsim 1.$$

The kernel decomposition condition (Assumption B.3) is satisfied by the patch-based multilevel decomposition (4.1), as discussed in [32, Section 5.1]. Finally, the triangle inequality-like property (Assumption B.4) is a direct consequence of [33, Lemma 5.4]; see also [30, Example C.3].

Given an initial guess  $\mathbf{u}^{(0)} \in V$ , we define

$$(4.7) \quad K_0 := \{\mathbf{v} \in V : F(\mathbf{v}) \leq F(\mathbf{u}^{(0)})\}.$$

Since all assumptions in Theorem B.5 have been verified, we obtain the following convergence result for Algorithm 3.1 by invoking that theorem.

THEOREM 4.3. *In Algorithm 4.1, assume that  $\tau \in (0, \tau_0]$ , where  $\tau_0$  was given in (4.2). Then there exists  $\zeta^* > 0$  such that, if  $F^\epsilon(\mathbf{u}^{(0)}) - F^\epsilon(\mathbf{u}_h^\epsilon) > \zeta^*$ , then*

$$F^\epsilon(\mathbf{u}^{(1)}) - F^\epsilon(\mathbf{u}_h^\epsilon) \leq \left(1 - \frac{\tau}{2}\right) (F^\epsilon(\mathbf{u}^{(0)}) - F^\epsilon(\mathbf{u}_h^\epsilon)),$$

and otherwise,

$$F^\epsilon(\mathbf{u}^{(n)}) - F^\epsilon(\mathbf{u}_h^\epsilon) \leq \frac{C_1^3}{\tau^3 C_2^2 n^3}, \quad n \geq 1,$$

where  $C_1$  is a positive constant independent of  $\epsilon$ , except for its implicit dependence on  $K_0$ , and  $C_2 = \min\{\mu_{0,K_0}, \mu_{1,K_0}\}$  (see (4.6)).

We note that the convergence theorem above explains how the convergence rate of Algorithm 4.1 depends on the augmented Lagrangian parameter  $\epsilon$ , but not explicitly on the mesh size  $h$ . In fact, the constant  $C_1$  in Theorem 4.3, which is defined in terms of stable decompositions of the multilevel subspaces (4.1) (see [30, Theorem 5.8]), may implicitly depend on  $h$ .



While  $h$ -independence of multilevel space decompositions for linear problems in  $H(\operatorname{div}; \Omega)$  has been established in the literature [2, 21] using the Helmholtz decomposition, extending these arguments to our setting is highly nontrivial. The main difficulty stems from the fact that our problem is posed on the space  $X = H(\operatorname{div}; \Omega) \cap L^3(\Omega)^d$ , which requires controlling the  $L^3(\Omega)^d$ -norm in addition to the  $H(\operatorname{div}; \Omega)$ -norm.

In section 5, we provide numerical evidence indicating that the convergence of Algorithm 4.1 is robust with respect to  $h$ , similarly to the case of linear problems, across a range of problem settings.

*Remark 4.4.* Combining Lemma 4.2(b) with the inverse inequality  $\|\mathbf{w}\|_{L^3(\Omega)} \lesssim h^{-\frac{d}{6}} \|\mathbf{w}\|_{L^2(\Omega)}$  [8, Theorem 4.5.11], we can verify that the local uniform convexity condition (Assumption B.2) holds with  $p = 2$ , although the constant  $\mu_{1,K}$  depends on the mesh size  $h$ . Consequently, by invoking Theorem B.5(a), we obtain the linear convergence of Algorithm 4.1. However, the resulting convergence rate is suboptimal due to its dependence on  $h$ , which originates from the inverse inequality.

*Remark 4.5.* In [44], an alternative approach was proposed for analyzing the  $\epsilon$ -independence of the convergence rate of subspace correction methods for solving problems of the form (3.1). However, to apply the strategy developed in [44], one must construct a stable decomposition for the multilevel spaces (4.1) that satisfies certain specific conditions [44, Assumption 3.1], which is not straightforward.

**4.3. Backtracking line search.** As stated in Theorem 4.3, the step size  $\tau$  must be chosen smaller than  $\tau_0$  given in (4.2) to guarantee the convergence of Algorithm 4.1. However, in this case, computing an explicit lower bound for  $\tau_0$  is needed, and any such estimate may be overly conservative, potentially resulting in slow convergence of Algorithm 4.1. To address this issue, we incorporate a backtracking line search strategy for selecting the step size, as introduced in [43], into the proposed multilevel method. The resulting algorithm is summarized in Algorithm 4.2.

The key idea behind the backtracking strategy is to adaptively select a step size  $\tau$  such that the global energy decay exceeds the sum of the local energy decays, weighted appropriately. It was shown in [43, Lemma 3.1] that the backtracking procedure always terminates, and a lower bound for  $\tau^{(n)}$  can be established in terms of  $\tau_0$  defined in (4.2). Therefore, Algorithm 4.2 does not require a priori knowledge of  $\tau_0$ .

Moreover, both theoretical and numerical results in [43] demonstrate that the backtracking strategy not only eliminates the need to tune the step size  $\tau$  but can also improve the convergence rate. The convergence analysis for the backtracking-enhanced method follows similar lines to the case without backtracking; we refer to [43] for details and omit it here.

**5. Numerical results.** In this section, we present numerical results for the proposed multilevel methods (Algorithms 4.1 and 4.2) for solving the Darcy–Forchheimer model. We also include results for the augmented Lagrangian method (Algorithm 3.1) to support our theoretical findings. All numerical experiments were conducted using MATLAB R2022b on a desktop equipped with an AMD Ryzen 5 5600X CPU (3.7 GHz, 6 cores), 40 GB RAM, and the Windows 10 Pro operating system.

For the Darcy–Forchheimer model (2.1), we set  $\Omega = (0, 1)^2 \subset \mathbb{R}^2$  and assume that  $\mathbf{K} = K\mathbf{I}$  for some positive scalar  $K$ . Following the settings commonly used in the literature on numerical methods for the Darcy–Forchheimer model, we take  $\mu = 1$ ,  $\rho = 1$ , and  $K = 1$  as in [34, 23, 40], and vary the Forchheimer coefficient  $\beta = 0, 10, 20, 30$ , as in [23, 34]. Note that the case  $\beta = 0$  corresponds to the linear Darcy model.

---

**Algorithm 4.2** Parallel multilevel method for solving (3.1) with backtracking
 

---

Choose  $\mathbf{u}^{(0)} \in V$  and  $\tau^{(0)} > 0$ .

**for**  $n = 0, 1, 2, \dots$  **do**

**for**  $k = 1, 2, \dots, J$  **do**

**for**  $i = 1, 2, \dots, n_k$  **do**

$\mathbf{w}_{k,i}^{(n+1)} = \arg \min_{\mathbf{w}_{k,i} \in V_k^i} F^\epsilon(\mathbf{u}^{(n)} + \mathbf{w}_{k,i})$

**end for**

**end for**

$\tau \leftarrow 2\tau^{(n)}$

**repeat**

$\mathbf{u}^{(n+1)} = \mathbf{u}^{(n)} + \tau \sum_{k=1}^J \sum_{i=1}^{n_k} \mathbf{w}_{k,i}^{(n+1)}$

**if**  $F^\epsilon(\mathbf{u}^{(n)}) - F^\epsilon(\mathbf{u}^{(n+1)}) < \tau \sum_{k=1}^J \sum_{i=1}^{n_k} (F^\epsilon(\mathbf{u}^{(n)}) - F^\epsilon(\mathbf{u}^{(n)} + \mathbf{w}_{k,i}^{(n+1)}))$  **then**

$\tau \leftarrow \frac{\tau}{2}$

**end if**

**until**  $F^\epsilon(\mathbf{u}^{(n)}) - F^\epsilon(\mathbf{u}^{(n+1)}) \geq \tau \sum_{k=1}^J \sum_{i=1}^{n_k} (F^\epsilon(\mathbf{u}^{(n)}) - F^\epsilon(\mathbf{u}^{(n)} + \mathbf{w}_{k,i}^{(n+1)}))$

$\tau^{(n+1)} = \tau$

**end for**

---

We consider the following two benchmark examples taken from [40].

*Example 5.1.* The functions  $\mathbf{f}$  and  $g$ , and the corresponding exact solutions  $\mathbf{u}$  and  $p$  of (2.1) are given by

$$\begin{aligned} \mathbf{f}(x, y) &= \left( \frac{\mu}{\rho K} + \frac{\beta}{\rho} e^x \right) (e^x \sin y, e^x \cos y)^T + (y(1-2x)(1-y), x(1-x)(1-2y))^T, \\ g(x, y) &= 0, \quad \mathbf{u}(x, y) = (e^x \sin y, e^x \cos y)^T, \quad p(x, y) = xy(1-x)(1-y). \end{aligned}$$

*Example 5.2.* The functions  $\mathbf{f}$  and  $g$ , and the corresponding exact solutions  $\mathbf{u}$  and  $p$  of (2.1) are given by

$$\begin{aligned} \mathbf{f}(x, y) &= \left( \frac{\mu}{\rho K} + \frac{\beta}{\rho} \sqrt{x^2 e^{2y} + y^2 e^{2x}} \right) (xe^y, ye^x)^T + \pi(\cos \pi x \sin \pi y, \sin \pi x \cos \pi y)^T, \\ g(x, y) &= e^x + e^y, \quad \mathbf{u}(x, y) = (xe^y, ye^x)^T, \quad p(x, y) = \sin \pi x \sin \pi y. \end{aligned}$$

In all experiments and for all algorithms, we use zero initial guesses. For the nearly semicoercive problem (3.1), we set  $q_h = 0$  throughout. In the linear case ( $\beta = 0$ ), we employ Algorithm 4.1 as a preconditioner for the conjugate gradient method [7].

**5.1. Augmented Lagrangian method.** Numerical results for the augmented Lagrangian method (Algorithm 3.1) for various values of the augmented Lagrangian parameter  $\epsilon$  and mesh size  $h$  for solving Examples 5.1 and 5.2 are presented in Tables 1 and 2, respectively. We use the stopping criterion

$$(5.1) \quad \max \left\{ \frac{\|\mathbf{u}_h^{(n)} - \mathbf{u}_h\|_{\ell^2}}{\|\mathbf{u}_h\|_{\ell^2}}, \frac{\|p_h^{(n)} - p_h\|_{\ell^2}}{\|p_h\|_{\ell^2}} \right\} < 10^{-3},$$

TABLE 1

Number of iterations required by the augmented Lagrangian method ([Algorithm 3.1](#)) to satisfy the stopping criterion (5.1), for various values of the augmented Lagrangian parameter  $\epsilon$  and mesh size  $h$  ([Example 5.1](#)).

$\beta = 0$					$\beta = 10$				
$\epsilon \backslash h$	$10^0$	$10^{-1}$	$10^{-2}$	$10^{-3}$	$\epsilon \backslash h$	$10^0$	$10^{-1}$	$10^{-2}$	$10^{-3}$
$2^{-4}$	3	2	1	1	$2^{-4}$	12	4	2	2
$2^{-5}$	3	2	1	1	$2^{-5}$	12	4	2	2
$2^{-6}$	3	2	1	1	$2^{-6}$	12	4	2	2
$2^{-7}$	3	2	1	1	$2^{-7}$	12	4	2	2

$\beta = 20$					$\beta = 30$				
$\epsilon \backslash h$	$10^0$	$10^{-1}$	$10^{-2}$	$10^{-3}$	$\epsilon \backslash h$	$10^0$	$10^{-1}$	$10^{-2}$	$10^{-3}$
$2^{-4}$	19	5	2	2	$2^{-4}$	27	6	3	2
$2^{-5}$	19	5	2	2	$2^{-5}$	26	6	3	2
$2^{-6}$	19	5	2	2	$2^{-6}$	27	6	3	2
$2^{-7}$	20	5	2	2	$2^{-7}$	27	6	3	2

TABLE 2

Number of iterations required by the augmented Lagrangian method ([Algorithm 3.1](#)) to satisfy the stopping criterion (5.1), for various values of the augmented Lagrangian parameter  $\epsilon$  and mesh size  $h$  ([Example 5.2](#)).

$\beta = 0$					$\beta = 10$				
$\epsilon \backslash h$	$10^0$	$10^{-1}$	$10^{-2}$	$10^{-3}$	$\epsilon \backslash h$	$10^0$	$10^{-1}$	$10^{-2}$	$10^{-3}$
$2^{-4}$	3	2	1	1	$2^{-4}$	9	3	2	1
$2^{-5}$	3	2	1	1	$2^{-5}$	9	3	2	1
$2^{-6}$	3	2	1	1	$2^{-6}$	9	3	2	1
$2^{-7}$	3	2	1	1	$2^{-7}$	9	3	2	1

$\beta = 20$					$\beta = 30$				
$\epsilon \backslash h$	$10^0$	$10^{-1}$	$10^{-2}$	$10^{-3}$	$\epsilon \backslash h$	$10^0$	$10^{-1}$	$10^{-2}$	$10^{-3}$
$2^{-4}$	15	4	2	2	$2^{-4}$	20	5	2	2
$2^{-5}$	15	4	2	2	$2^{-5}$	20	5	2	2
$2^{-6}$	15	4	2	2	$2^{-6}$	20	5	2	2
$2^{-7}$	15	4	2	2	$2^{-7}$	20	5	2	2

where  $\|\cdot\|_{\ell^2}$  denotes the standard  $\ell^2$ -norm of the vector of degrees of freedom.

In all cases, we observe that the number of iterations decreases as  $\epsilon$  decreases, in agreement with [Theorem 3.1](#). Moreover, the number of iterations remains uniformly bounded as the mesh is refined. Hence, we conclude that [Algorithm 3.1](#) converges in very few iterations even for small values of  $h$ , provided that  $\epsilon$  is sufficiently small. These results support our claim that the mixed problem (2.5) can be reduced to the optimization problem (3.1).

**5.2. Backtracking line search.** To observe the effect of the backtracking strategy introduced in [Algorithm 4.2](#), we present convergence curves for the multilevel

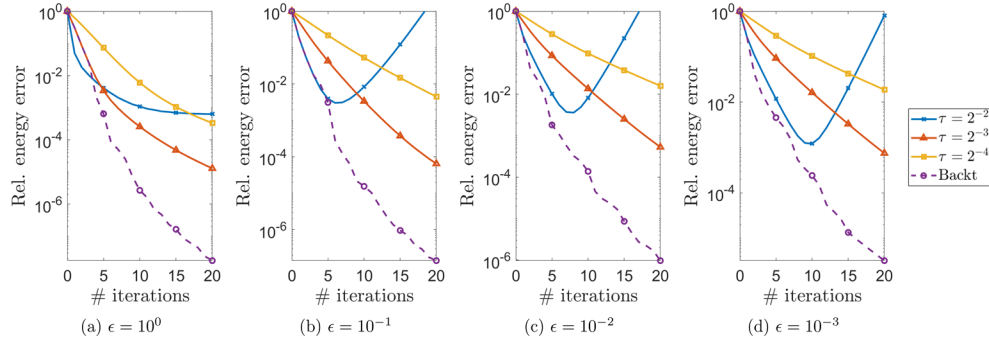


FIG. 2. Convergence curves of the relative energy error  $\frac{F^\epsilon(\mathbf{u}^{(n)}) - \min F^\epsilon}{|\min F^\epsilon|}$  for the proposed multilevel method (Algorithm 4.1) with step sizes  $\tau = 2^{-2}, 2^{-3}, 2^{-4}$ , and for the proposed multilevel method with backtracking (Algorithm 4.2), shown for various values of the augmented Lagrangian parameter  $\epsilon$ . Curves for Algorithm 4.1 are plotted in solid lines, while the curve for Algorithm 4.2 is plotted in dashed line (Example 5.1,  $\beta = 30$ ,  $h = 2^{-5}$ ).

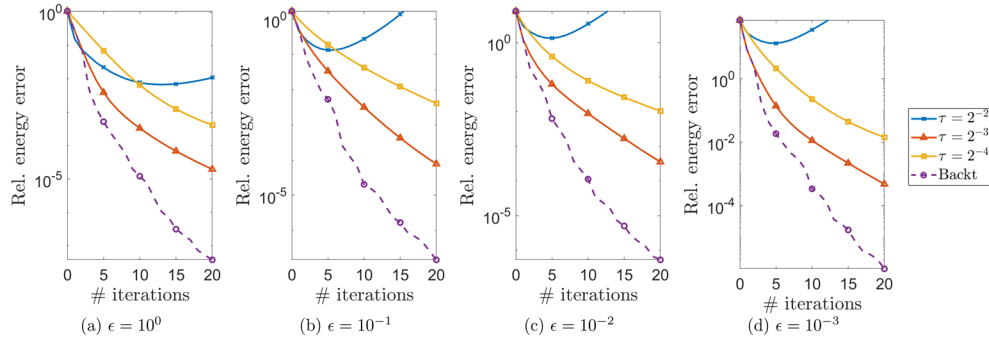


FIG. 3. Convergence curves of the relative energy error  $\frac{F^\epsilon(\mathbf{u}^{(n)}) - \min F^\epsilon}{|\min F^\epsilon|}$  for the proposed multilevel method (Algorithm 4.1) with step sizes  $\tau = 2^{-2}, 2^{-3}, 2^{-4}$ , and for the proposed multilevel method with backtracking (Algorithm 4.2), shown for various values of the augmented Lagrangian parameter  $\epsilon$ . Curves for Algorithm 4.1 are plotted in solid lines, while the curve for Algorithm 4.2 is plotted in dashed line (Example 5.2,  $\beta = 30$ ,  $h = 2^{-5}$ ).

methods Algorithms 4.1 and 4.2 in Figures 2 and 3, where step sizes  $\tau = 2^{-2}, 2^{-3}, 2^{-4}$  are used for Algorithm 4.1. For Algorithm 4.1, we observe that when the step size is set to  $\tau = 2^{-2}$ , the algorithm diverges in almost all cases, indicating that overly large step sizes may lead to divergence. For smaller step sizes  $\tau \leq 2^{-3}$ , the algorithm converges in all cases, and larger step sizes among them result in faster convergence. This implies that, provided  $\tau$  is sufficiently small to ensure convergence, larger values within the admissible range yield better performance.

In contrast, for Algorithm 4.2, which adaptively determines the step size using the backtracking scheme, we consistently observe superior convergence rates across all test cases when compared to Algorithm 4.1. This demonstrates the effectiveness of the backtracking strategy in improving convergence behavior.

Based on these observations, we focus exclusively on Algorithm 4.2 in the re-

TABLE 3

Minimum step size  $\min_{n \geq 0} \tau^{(n)}$  in the proposed multilevel method with backtracking (Algorithm 4.2) in the numerical experiments corresponding to Figures 2 and 3.

$\epsilon = 10^0$	$\epsilon = 10^{-1}$	$\epsilon = 10^{-2}$	$\epsilon = 10^{-3}$	$\epsilon = 10^0$	$\epsilon = 10^{-1}$	$\epsilon = 10^{-2}$	$\epsilon = 10^{-3}$
$2^{-3}$	$2^{-3}$	$2^{-3}$	$2^{-4}$	$2^{-3}$	$2^{-3}$	$2^{-3}$	$2^{-3}$

(a) Example 5.1

$\epsilon = 10^0$	$\epsilon = 10^{-1}$	$\epsilon = 10^{-2}$	$\epsilon = 10^{-3}$
$2^{-3}$	$2^{-3}$	$2^{-3}$	$2^{-3}$

(a) Example 5.2

TABLE 4

Number of iterations required by the proposed multilevel method (Algorithm 4.2) to satisfy the stopping criterion (5.2), for various values of the augmented Lagrangian parameter  $\epsilon$  and mesh size  $h$  (Example 5.1).

$\beta = 0$				
$\epsilon \backslash h$	$10^0$	$10^{-1}$	$10^{-2}$	$10^{-3}$
$2^{-4}$	5	5	5	4
$2^{-5}$	5	5	5	5
$2^{-6}$	5	5	5	5
$2^{-7}$	5	5	5	5

$\beta = 10$				
$\epsilon \backslash h$	$10^0$	$10^{-1}$	$10^{-2}$	$10^{-3}$
$2^{-4}$	5	6	8	7
$2^{-5}$	5	7	7	7
$2^{-6}$	5	9	9	9
$2^{-7}$	5	9	9	9

$\beta = 20$				
$\epsilon \backslash h$	$10^0$	$10^{-1}$	$10^{-2}$	$10^{-3}$
$2^{-4}$	4	7	8	7
$2^{-5}$	4	7	7	8
$2^{-6}$	4	8	8	9
$2^{-7}$	5	8	9	9

$\beta = 30$				
$\epsilon \backslash h$	$10^0$	$10^{-1}$	$10^{-2}$	$10^{-3}$
$2^{-4}$	4	6	7	7
$2^{-5}$	5	6	7	8
$2^{-6}$	5	7	8	9
$2^{-7}$	5	7	9	9

maining numerical experiments, as it consistently outperforms Algorithm 4.1 in all scenarios considered.

On the other hand, the minimum step sizes  $\min_{n \geq 0} \tau^{(n)}$  in Algorithm 4.2 are presented in Table 3. We see that the minimum step size does not decrease significantly even if the augmented Lagrangian parameter  $\epsilon$  becomes small. This implies that the backtracking scheme is robust with respect to the nearly semicoercive behavior of the problem (3.1).

**5.3. Dependence on  $\epsilon$  and  $h$ .** Finally, to observe the robustness of Algorithm 4.2 with respect to the augmented Lagrangian parameter  $\epsilon$  and the mesh size  $h$ , we present numerical results of Algorithm 4.2 for various values of  $\epsilon$  and  $h$  solving Examples 5.1 and 5.2 in Tables 4 and 5, respectively, where the following stopping criterion is used:

$$(5.2) \quad \frac{F^\epsilon(\mathbf{u}^{(n)}) - \min F^\epsilon}{|\min F^\epsilon|} < 10^{-3}.$$

We observe that the number of iterations does not increase significantly even if either  $\epsilon$  or  $h$  becomes small, which aligns with Theorem 4.3. That is, the performance of Algorithm 4.2 is robust even when the nearly semicoercive behavior of the problem (3.1) is strong and the scale of the discretized problem is large.

**6. Concluding remarks.** In this paper, we proposed multilevel methods for solving the Darcy–Forchheimer model based on a nearly semicoercive formulation.

TABLE 5

Number of iterations required by the proposed multilevel method ([Algorithm 4.2](#)) to satisfy the stopping criterion ([5.2](#)), for various values of the augmented Lagrangian parameter  $\epsilon$  and mesh size  $h$  ([Example 5.2](#)).

$\beta = 0$					$\beta = 10$				
$\epsilon \backslash h$	$10^0$	$10^{-1}$	$10^{-2}$	$10^{-3}$	$\epsilon \backslash h$	$10^0$	$10^{-1}$	$10^{-2}$	$10^{-3}$
$2^{-4}$	6	5	4	4	$2^{-4}$	5	8	9	10
$2^{-5}$	6	5	4	4	$2^{-5}$	6	7	10	9
$2^{-6}$	6	6	4	4	$2^{-6}$	6	9	11	11
$2^{-7}$	6	6	4	4	$2^{-7}$	6	10	12	12

$\beta = 20$					$\beta = 30$				
$\epsilon \backslash h$	$10^0$	$10^{-1}$	$10^{-2}$	$10^{-3}$	$\epsilon \backslash h$	$10^0$	$10^{-1}$	$10^{-2}$	$10^{-3}$
$2^{-4}$	5	7	9	10	$2^{-4}$	5	7	8	9
$2^{-5}$	5	7	8	9	$2^{-5}$	5	7	8	10
$2^{-6}$	5	8	10	11	$2^{-6}$	5	8	10	11
$2^{-7}$	5	9	11	12	$2^{-7}$	5	8	11	12

We first proved that the Darcy–Forchheimer model, formulated as a mixed problem, can be reduced to a nearly semicoercive convex optimization problem via the augmented Lagrangian method. Then, based on this nearly semicoercive formulation, we developed a multilevel method utilizing multilevel patch-based space decomposition, with convergence analysis demonstrating robustness with respect to the augmented Lagrangian parameter  $\epsilon$ . Additionally, we introduced a backtracking scheme for line search within the proposed multilevel method.

This work opens several interesting directions for future research. The first direction concerns rigorous mathematical analysis of the convergence behavior of the proposed multilevel methods with respect to the mesh size  $h$ . While the  $h$ -independent convergence rate of parallel multilevel methods for linear problems has been extensively studied in the literature (e.g., [\[53, 54\]](#)), extending these results to our nonlinear setting poses significant challenges. One major difficulty lies in controlling the  $L^3(\Omega)^d$ -norm in addition to the  $H(\text{div}; \Omega)$ -norm, as discussed in [section 4](#).

Another interesting direction is the improvement of the algorithm. Although the convergence rates of the proposed multilevel methods are close to optimal, the computational cost per iteration could be further reduced by adopting the full approximation scheme [\[9, 11\]](#), which fully decouples the global and local degrees of freedom in the computation. This improvement will be considered in future work.

#### Appendix A. Convergence analysis of the augmented Lagrangian method.

In this appendix, we present a proof of [Theorem 3.1](#) in an abstract setting. That is, we provide a convergence rate analysis of the augmented Lagrangian method [\[20, 45\]](#) for solving convex optimization problems with linear constraints.

Let  $V$  and  $W$  be finite-dimensional real vector spaces equipped with inner products  $(\cdot, \cdot)$  and associated norms  $\|\cdot\|$ . We consider the following general convex optimization problem with a linear constraint:

$$(A.1) \quad \min_{v \in V} F(v) \quad \text{subject to} \quad Bv = g,$$

where  $B: V \rightarrow W$  is a linear operator,  $F: V \rightarrow \overline{\mathbb{R}}$  is a convex functional, and  $g \in W$ . Let  $u \in V$  denote a solution to (A.1). The augmented Lagrangian method for solving (A.1) is summarized in Algorithm A.1.

---

**Algorithm A.1** Augmented Lagrangian method for solving (A.1)

---

Given  $\epsilon > 0$ :  
 Choose  $p^{(0)} \in W$ .  
**for**  $n = 0, 1, 2, \dots$  **do**  
 $u^{(n+1)} = \arg \min_{v \in V} \left\{ F(v) + (p^{(n)}, Bv - g) + \frac{1}{2\epsilon} \|Bv - g\|^2 \right\}$   
 $p^{(n+1)} = p^{(n)} + \epsilon^{-1} (Bu^{(n+1)} - g)$   
**end for**

---

We observe that Algorithm A.1 reduces to Algorithm 3.1 if we set  
 (A.2)  $V \leftarrow X_h, \quad W \leftarrow M_h, \quad \|\cdot\| \leftarrow \|\cdot\|_{L^2(\Omega)}, \quad F(v) \leftarrow F(v), \quad B \leftarrow -\operatorname{div}, \quad g \leftarrow -g_h.$

To carry out the convergence analysis, we leverage the equivalence between the augmented Lagrangian method and the proximal point algorithm [35, 47] for solving a dual problem, as established in [24, 50]. By invoking Fenchel–Rockafellar duality [46], the dual problem associated with (A.1) is given by

$$(A.3) \quad \min_{q \in W} \{F^*(-B^*q) + (g, q)\},$$

where  $B^*: W \rightarrow V$  denotes the adjoint of  $B$ , and  $F^*: V \rightarrow \overline{\mathbb{R}}$  is the Legendre–Fenchel conjugate of  $F$ , defined by

$$(A.4) \quad F^*(w) = \sup_{v \in V} \{(w, v) - F(v)\}, \quad w \in V.$$

The proximal point algorithm for solving (A.3) is summarized in Algorithm A.2.

---

**Algorithm A.2** Proximal point algorithm for solving (A.1)

---

Given  $\epsilon > 0$ :  
 Choose  $q^{(0)} \in W$ .  
**for**  $n = 0, 1, 2, \dots$  **do**  
 $q^{(n+1)} = \arg \min_{q \in W} \left\{ F^*(-B^*q) + (g, q) + \frac{\epsilon}{2} \|q - q^{(n)}\|^2 \right\}$   
**end for**

---

In Lemma A.1, we summarize the equivalence between Algorithms A.1 and A.2; see [24, Remark 6.2] for details.

LEMMA A.1. *The augmented Lagrangian method presented in Algorithm A.1 is equivalent to the proximal point algorithm presented in Algorithm A.2 in the following sense: if  $p^{(0)} = q^{(0)}$ , then we have  $p^{(n)} = q^{(n)}$  for all  $n \geq 0$ .*

Thanks to Lemma A.1, it suffices to analyze Algorithm A.2 in order to establish the convergence rate of Algorithm A.1. In Lemma A.2, we present the convergence result for the proximal point algorithm, as established in [4, Example 23.40]; see also [25, 47].

LEMMA A.2. In (A.3), suppose that  $F^* \circ (-B^*)$  is  $\mu$ -strongly convex for some  $\mu > 0$ , ensuring that (A.3) admits a unique solution  $p \in W$ . Then, in the proximal point algorithm presented in Algorithm A.2, we have

$$\|q^{(n+1)} - p\| \leq \frac{\epsilon}{\mu + \epsilon} \|q^{(n)} - p\|, \quad n \geq 0.$$

Remark A.3. For certain convex optimization problems of the form (A.3) arising in partial differential equations (see, e.g., [29]), particularly the dual problem associated with (2.6), the composition  $F^* \circ (-B^*)$  is only *locally* strongly convex. Nevertheless, since Algorithm A.2 is a contraction, the sequence  $\{q^{(n)}\}$  remains bounded. This boundedness allows the assumption of global strong convexity in Lemma A.2 to be relaxed to a local one. For simplicity and clarity of the analysis, however, we continue to assume global strong convexity throughout. A related discussion appears in [51, Remark 2.1].

Using Lemmas A.1 and A.2, we establish the convergence rate of Algorithm A.1, as stated in Theorem A.4. We remark that Theorem A.4 generalizes [32, Lemma 2.1], which addresses the special case where  $F$  is quadratic, i.e., when (A.1) reduces to a linear saddle-point problem. In Theorem A.4,  $D_F^{\text{sym}}$  denotes the *symmetrized Bregman divergence* associated with  $F$  [1, 39], defined by

$$(A.5) \quad D_F^{\text{sym}}(v, w) = (\nabla F(v) - \nabla F(w), v - w), \quad v, w \in V.$$

THEOREM A.4. In (A.3), suppose that  $F^* \circ (-B^*)$  is  $\mu$ -strongly convex. Then, in the augmented Lagrangian method presented in Algorithm A.1, we have

$$(A.6) \quad \|p^{(n+1)} - p\| \leq \frac{\epsilon}{\mu + \epsilon} \|p^{(n)} - p\|, \quad n \geq 0.$$

Moreover, if we further assume that  $F$  is differentiable, then we have

$$(A.7) \quad D_F^{\text{sym}}(u^{(n+1)}, u) \leq \begin{cases} \frac{\mu \epsilon^2}{(\mu + \epsilon)^2} \|p^{(n)} - p\|^2, & \text{if } \epsilon \leq \mu, \\ \frac{\epsilon}{4} \|p^{(n)} - p\|^2, & \text{if } \epsilon > \mu, \end{cases} \quad n \geq 0.$$

*Proof.* The first estimate (A.6) follows obviously from Lemmas A.1 and A.2. To prove (A.7), we first see that the optimality condition for (A.1) reads as

$$(A.8a) \quad \nabla F(u) + B^* p = 0,$$

$$(A.8b) \quad Bu = g.$$

Moreover, Algorithm A.1 reads as

$$(A.9a) \quad \nabla F(u^{(n+1)}) + B^* p^{(n)} + \epsilon^{-1} B^* (Bu^{(n+1)} - g) = 0,$$

$$(A.9b) \quad p^{(n+1)} = p^{(n)} + \epsilon^{-1} (Bu^{(n+1)} - g).$$

Combining (A.8a), (A.8b), and (A.9a) yields

$$(A.10) \quad \nabla F(u^{(n+1)}) - \nabla F(u) + B^* (p^{(n)} - p) + \epsilon^{-1} B^* B(u^{(n+1)} - u) = 0.$$

In addition, combining (A.8b) and (A.9b) yields

$$(A.11) \quad p^{(n+1)} - p^{(n)} = \epsilon^{-1} B(u^{(n+1)} - u).$$



It follows that

$$\begin{aligned}
 D_F^{\text{sym}}(u^{(n+1)}, u) &\stackrel{\text{(A.5)}}{=} (\nabla F(u^{(n+1)}) - \nabla F(u), u^{(n+1)} - u) \\
 &\stackrel{\text{(A.10)}}{=} -(B^*(p^{(n)} - p), u^{(n+1)} - u) - \epsilon^{-1}(B^*B(u^{(n+1)} - u), u^{(n+1)} - u) \\
 (A.12) \quad &\stackrel{\text{(A.11)}}{=} -\epsilon \|p^{(n+1)} - p\|^2 + \epsilon(p^{(n+1)} - p, p^{(n)} - p) \\
 &\leq \epsilon \left( \frac{1}{2\theta} - 1 \right) \|p^{(n+1)} - p\|^2 + \frac{\epsilon\theta}{2} \|p^{(n)} - p\|^2,
 \end{aligned}$$

where  $\theta$  is any positive real number. On one hand, if  $\epsilon \leq \mu$ , setting  $\theta = \frac{\epsilon}{\mu + \epsilon} \leq \frac{1}{2}$  in (A.12) yields

$$D_F^{\text{sym}}(u^{(n+1)}, u) \leq \frac{\mu - \epsilon}{2} \|p^{(n+1)} - p\|^2 + \frac{\epsilon^2}{2(\mu + \epsilon)} \|p^{(n)} - p\|^2 \stackrel{\text{(A.6)}}{\leq} \frac{\mu\epsilon^2}{(\mu + \epsilon)^2} \|p^{(n)} - p\|^2.$$

On the other hand, if  $\epsilon > \mu$ , setting  $\theta = \frac{1}{2}$  in (A.12) yields

$$D_F^{\text{sym}}(u^{(n+1)}, u) \leq \frac{\epsilon}{4} \|p^{(n)} - p\|^2.$$

This completes the proof.  $\square$

**Appendix B. Abstract theory of subspace correction methods for nearly semicoercive problems.** In this appendix, we provide a brief summary of the abstract convergence theory of subspace correction methods for nearly semicoercive convex optimization problems, as developed in [30]. Although the theory in [30] is formulated in a broader setting, we confine our discussion here to a specific case suitable for our purpose, for the sake of simplicity and clarity.

Let  $V$  be a uniformly smooth and uniformly convex Banach space (cf. [37]) equipped with a norm  $\|\cdot\|$  and a continuous seminorm  $|\cdot|$ . We consider the following nearly semicoercive model problem:

$$(B.1) \quad \min_{v \in V} \{F(v) := F_0(v) + \epsilon F_1(v)\},$$

where  $F_0: V \rightarrow \mathbb{R}$  and  $F_1: V \rightarrow \mathbb{R}$  are Gâteaux differentiable and convex functionals, and  $\epsilon$  is a small positive parameter, say  $\epsilon \in (0, 1/2]$ . We further assume that  $F_0$  is semicoercive with respect to  $|\cdot|$  [30, Proposition 2.3], and that  $F_1$  is coercive.

Suppose that the space  $V$  admits the following space decomposition:

$$(B.2) \quad V = \sum_{k=1}^J V_k,$$

where each  $V_k$ ,  $1 \leq k \leq J$ , is a closed subspace of  $V$ . The strengthened convexity condition [30, Equation (3.4)] asserts that there exists a constant  $\tau_0 > 0$  such that

$$(B.3) \quad (1 - \tau_0)F(v) + \tau_0 \sum_{k=1}^J F(v + w_k) \geq F\left(v + \tau_0 \sum_{k=1}^J w_k\right), \quad v \in V, w_k \in V_k.$$

The parallel subspace correction method for solving the problem (B.1) based on the space decomposition (B.2) is presented in B.1.

**Algorithm B.1** Parallel subspace correction method for solving (B.1)

---

Given  $\tau > 0$ :  
 Choose  $u^{(0)} \in V$ .  
**for**  $n = 0, 1, 2, \dots$  **do**  
     **for**  $k = 1, 2, \dots, N$  **do**  
          $w_k^{(n+1)} = \arg \min_{w_k \in V_k} F(u^{(n)} + w_k)$   
     **end for**  
      $u^{(n+1)} = u^{(n)} + \tau \sum_{k=1}^J w_k^{(n+1)}$   
**end for**

---

In the following, we present conditions that should be verified to show convergence of Algorithm B.1. We define the Bregman divergences  $d_0$  and  $d_1$  corresponding to  $F_0$  and  $F_1$ , respectively, as in (4.4). Combination of [30, Proposition 4.9 and Assumption 5.4] yields the following local smoothness condition.

*Assumption B.1* (local smoothness). For any  $\|\cdot\|$ -bounded and convex subset  $K$  of  $V$ , we have

$$\sup_{v, v+w \in K} \frac{d_0(w; v)}{\|w\|^2} < \infty \quad \text{and} \quad \sup_{v, v+w \in K} \frac{d_1(w; v)}{\|w\|^2} < \infty.$$

The local uniform convexity condition [30, Assumption 5.9] is presented as follows.

*Assumption B.2* (local uniform convexity). For some  $p \geq 2$ , we have the following:

(a) For any  $\|\cdot\|$ -bounded and convex subset  $K$  of  $V$ , we have

$$\mu_{0,K} := \inf_{v, v+w \in K} \frac{d_0(w; v)}{\|w\|^p} > 0.$$

(b) For any  $\|\cdot\|$ -bounded and convex subset  $K$  of  $V$ , we have

$$\mu_{1,K} := \inf_{v, v+w \in K} \frac{(d_0 + d_1)(w; v)}{\|w\|^p} > 0.$$

Under Assumptions B.1 and B.2, we can ensure convergence of Algorithm B.1 [30, Theorem 4.13] (see also [42, Theorem 4.8]). However, in order to ensure  $\epsilon$ -dependent convergence rate, we need more conditions.

The following kernel decomposition assumption [30, Assumption 5.6], originally introduced in [32] for the analysis of linear problems, plays a critical role in the convergence theory.

*Assumption B.3* (kernel decomposition). The kernel  $\mathcal{N} = \ker F_0$  of the semicoercive functional  $F_0$  in (B.1) admits the decomposition

$$\mathcal{N} = \sum_{k=1}^J (V_k \cap \mathcal{N}).$$

The next condition, Assumption B.4, describes a triangle-inequality-like property stated in [30, Assumption 5.7].

*Assumption B.4* (triangle inequality-like property). For any bounded and convex subset  $K \subset V$ , there exists a constant  $C_K > 0$  such that

$$(B.4) \quad d_1(w + w'; v) \leq C_K (d_1(w; v) + d_1(w'; v)), \quad v \in K, \quad w, w' \in V.$$

Similar to (4.7), given an initial guess  $u^{(0)} \in V$  for [Algorithm B.1](#), we define the set  $K_0$  by

$$(B.5) \quad K_0 := \{v \in V : F(v) \leq F(u^{(0)})\}.$$

Note that  $K_0$  depends implicitly on  $\epsilon$  due to the  $\epsilon$ -dependence of the energy functional  $F$ ; see [30, Remark 5.5]. Under all the assumptions stated above, we obtain the following convergence theorem, which is a direct consequence of [30, Theorems 4.13, 5.8, and 5.10].

**THEOREM B.5.** *Suppose that [Assumptions B.1 to B.4](#) hold. In [Algorithm B.1](#), assume that  $\tau \in (0, \tau_0]$ , where  $\tau_0$  was given in (B.3). Then we have the following:*

(a) *In the case  $p = 2$ , we have*

$$F(u^{(n)}) - F(u) \leq \left(1 - \frac{\tau}{2} \min \left\{1, \frac{C_2}{C_1}\right\}\right)^n (F(u^{(0)}) - F(u)), \quad n \geq 0,$$

*where  $C_1$  is a positive constant independent of  $\epsilon$ , except for its implicit dependence on  $K_0$  (see (B.5)), and  $C_2 = \min\{\mu_{0,K_0}, \mu_{1,K_0}\}$ .*

(b) *In the case  $p > 2$ , there exists  $\zeta^* > 0$  such that, if  $F(u^{(0)}) - F(u) > \zeta^*$ , then*

$$F(u^{(1)}) - F(u) \leq \left(1 - \frac{\tau}{2}\right) (F(u^{(0)}) - F(u)),$$

*and otherwise,*

$$F(u^{(n)}) - F(u) \leq \frac{C_1^{\frac{p}{p-2}}}{\tau^{\frac{p}{p-2}} C_2^{\frac{2}{p-2}} n^{\frac{p}{p-2}}}, \quad n \geq 1,$$

*where  $C_1$  and  $C_2$  are as defined in (a).*

## REFERENCES

- [1] S. ACHARYYA, A. BANERJEE, AND D. BOLEY, *Bregman divergences and triangle inequality*, in Proceedings of the 2013 SIAM International Conference on Data Mining (SDM), Society for Industrial and Applied Mathematics (SIAM), Philadelphia, PA, 2013, pp. 476–484.
- [2] D. N. ARNOLD, R. S. FALK, AND R. WINTHER, *Multigrid in  $H(\text{div})$  and  $H(\text{curl})$* , Numer. Math., 85 (2000), pp. 197–217.
- [3] A. ARRARÁS, F. J. GASPAR, L. PORTERO, AND C. RODRIGO, *Geometric multigrid methods for Darcy–Forchheimer flow in fractured porous media*, Comput. Math. Appl., 78 (2019), pp. 3139–3151.
- [4] H. H. BAUSCHKE AND P. L. COMBETTES, *Convex Analysis and Monotone Operator Theory in Hilbert Spaces*, Springer, New York, 2011.
- [5] D. BOFFI, F. BREZZI, AND M. FORTIN, *Mixed Finite Element Methods and Applications*, Springer, Heidelberg, 2013.
- [6] S. BOYD AND L. VANDENBERGHE, *Convex Optimization*, Cambridge University Press, Cambridge, 2004.
- [7] J. H. BRAMBLE, J. E. PASCIAK, AND J. XU, *Parallel multilevel preconditioners*, Math. Comp., 55 (1990), pp. 1–22.
- [8] S. C. BRENNER AND L. R. SCOTT, *The Mathematical Theory of Finite Element Methods*, Springer, New York, third ed., 2008.

- [9] E. BUELER AND P. E. FARRELL, *A full approximation scheme multilevel method for nonlinear variational inequalities*, SIAM J. Sci. Comput., 46 (2024), pp. A2421–A2444.
- [10] L. CHEN, R. GUO, AND J. WEI, *Transformed primal-dual methods with variable-preconditioners*, arXiv preprint arXiv:2312.12355, (2023).
- [11] L. CHEN, X. HU, AND S. WISE, *Convergence analysis of the fast subspace descent method for convex optimization problems*, Math. Comp., 89 (2020), pp. 2249–2282.
- [12] Z. CHEN, Y. DING, Z. QIN, Y. HE, B. LIANG, Y. QING, Y. XING, AND B. LI, *Effects of high-velocity flow on the temperature field near the wellbore: A review*, in 2023 International Conference on Energy Engineering, Springer, 2023, pp. 887–912.
- [13] P. G. CIARLET, *The Finite Element Method for Elliptic Problems*, Society for Industrial and Applied Mathematics (SIAM), Philadelphia, PA, 2002.
- [14] M. DRYJA, M. V. SARKIS, AND O. B. WIDLUND, *Multilevel Schwarz methods for elliptic problems with discontinuous coefficients in three dimensions*, Numer. Math., 72 (1996), pp. 313–348.
- [15] F. A. FAIRAG AND J. D. AUDU, *Two-level Galerkin mixed finite element method for Darcy–Forchheimer model in porous media*, SIAM J. Numer. Anal., 58 (2020), pp. 234–253.
- [16] A. GAVASKAR, N. GUPTA, B. SASS, R. JANOSY, AND J. HICKS, *Design guidance for application of permeable reactive barriers for groundwater remediation*, tech. report, BATTELLE Project Report, 2000.
- [17] V. GIRAULT AND M. F. WHEELER, *Numerical discretization of a Darcy–Forchheimer model*, Numer. Math., 110 (2008), pp. 161–198.
- [18] R. GOEBEL AND R. T. ROCKAFELLAR, *Local strong convexity and local Lipschitz continuity of the gradient of convex functions*, J. Convex Anal., 15 (2008), p. 263.
- [19] S. M. HASSANIZADEH AND W. G. GRAY, *High velocity flow in porous media*, Transp. Porous Media, 2 (1987), pp. 521–531.
- [20] M. R. HESTENES, *Multiplier and gradient methods*, J. Optim. Theory Appl., 4 (1969), pp. 303–320.
- [21] R. HIPTMAIR AND A. TOSELLI, *Overlapping and multilevel Schwarz methods for vector valued elliptic problems in three dimensions*, in Parallel Solution of Partial Differential Equations (Minneapolis, MN, 1997), vol. 120 of IMA Vol. Math. Appl., Springer, New York, 2000, pp. 181–208.
- [22] T. HORNEBER, C. RAUH, AND A. DELGADO, *Fluid dynamic characterisation of porous solids in catalytic fixed-bed reactors*, Micropor. Mesopor. Mat., 154 (2012), pp. 170–174.
- [23] J. HUANG, L. CHEN, AND H. RUI, *Multigrid methods for a mixed finite element method of the Darcy–Forchheimer model*, J. Sci. Comput., 74 (2018), pp. 396–411.
- [24] B. JIANG, J. PARK, AND J. XU, *Connections between convex optimization algorithms and subspace correction methods*, arXiv preprint arXiv:2505.09765, (2025).
- [25] D. KIM, *Accelerated proximal point method for maximally monotone operators*, Math. Program., 190 (2021), pp. 57–87.
- [26] E. L. KUNIANSKY, *Simulating groundwater flow in karst aquifers with distributed parameter models—Comparison of porous-equivalent media and hybrid flow approaches*, tech. report, US Geological Survey, 2016.
- [27] C.-O. LEE AND E.-H. PARK, *A dual iterative substructuring method with a penalty term*, Numer. Math., 112 (2009), pp. 89–113.
- [28] C.-O. LEE AND E.-H. PARK, *A dual iterative substructuring method with a small penalty parameter*, J. Korean Math. Soc., 54 (2017), pp. 461–477.
- [29] Y.-J. LEE AND J. PARK, *On the linear convergence of additive Schwarz methods for the  $p$ -Laplacian*, IMA J. Numer. Anal., (2024), p. drae068, <https://doi.org/10.1093/imanum/drae068>.
- [30] Y.-J. LEE AND J. PARK, *Subspace correction methods for semicoercive and nearly semicoercive convex optimization with applications to nonlinear PDEs*, arXiv preprint arXiv:2412.17318, (2024).
- [31] Y.-J. LEE, J. WU, AND J. CHEN, *Robust multigrid method for the planar linear elasticity problems*, Numer. Math., 113 (2009), pp. 473–496.
- [32] Y.-J. LEE, J. WU, J. XU, AND L. ZIKATANOV, *Robust subspace correction methods for nearly singular systems*, Math. Models Methods Appl. Sci., 17 (2007), pp. 1937–1963.
- [33] W. LIU AND N. YAN, *Quasi-norm local error estimators for  $p$ -Laplacian*, SIAM J. Numer. Anal., 39 (2001), pp. 100–127.
- [34] H. LÓPEZ, B. MOLINA, AND J. J. SALAS, *Comparison between different numerical discretizations for a Darcy–Forchheimer model*, Electron. Trans. Numer. Anal., 34 (2009), pp. 187–203.
- [35] B. MARTINET, *Régularisation d’inéquations variationnelles par approximations successives*, Rev. Française Informat. Recherche Opérationnelle, 4 (1970), pp. 154–158.

- [36] G. MEDICI AND L. J. WEST, *Groundwater flow velocities in karst aquifers; importance of spatial observation scale and hydraulic testing for contaminant transport prediction*, Environ. Sci. Pollut. Res. Int., 28 (2021), pp. 43050–43063.
- [37] R. E. MEGGINSON, *An Introduction to Banach Space Theory*, Springer-Verlag, New York, 1998.
- [38] H. MUSTAPHA, L. DE LANGAVANT, AND M. A. GIDDINS, *Darcy and non-Darcy flows in fractured gas reservoirs*, in SPE Reservoir Characterisation and Simulation Conference and Exhibition, SPE, 2015, p. D021S019R001.
- [39] F. NIELSEN AND R. NOCK, *Sided and symmetrized Bregman centroids*, IEEE Trans. Inform. Theory, 55 (2009), pp. 2882–2904.
- [40] H. PAN AND H. RUI, *Mixed element method for two-dimensional Darcy–Forchheimer model*, J. Sci. Comput., 52 (2012), pp. 563–587.
- [41] E.-J. PARK, *Mixed finite element methods for generalized Forchheimer flow in porous media*, Numer. Methods Partial Differential Equations, 21 (2005), pp. 213–228.
- [42] J. PARK, *Additive Schwarz methods for convex optimization as gradient methods*, SIAM J. Numer. Anal., 58 (2020), pp. 1495–1530.
- [43] J. PARK, *Additive Schwarz methods for convex optimization with backtracking*, Comput. Math. Appl., 113 (2022), pp. 332–344.
- [44] J. PARK, *Additive Schwarz methods for semilinear elliptic problems with convex energy functionals: Convergence rate independent of nonlinearity*, SIAM J. Sci. Comput., 46 (2024), pp. A1373–A1396.
- [45] M. J. D. POWELL, *A method for nonlinear constraints in minimization problems*, in Optimization (Sympos., Univ. Keele, Keele, 1968), Academic Press, London-New York, 1969, pp. 283–298.
- [46] R. T. ROCKAFELLAR, *Convex Analysis*, Princeton University Press, Princeton, NJ, 1970.
- [47] R. T. ROCKAFELLAR, *Monotone operators and the proximal point algorithm*, SIAM J. Control Optim., 14 (1976), pp. 877–898.
- [48] J. J. SALAS, H. LÓPEZ, AND B. MOLINA, *An analysis of a mixed finite element method for a Darcy–Forchheimer model*, Math. Comput. Model., 57 (2013), pp. 2325–2338.
- [49] M. SEDGHI-ASL, E. MORALES-CASIQUE, AND S. M. HASSANIZADEH, *Dispersion in high-porosity porous medium*, J. Porous Media, 26 (2023), pp. 1–12.
- [50] S. SETZER, *Operator splittings, Bregman methods and frame shrinkage in image processing*, Int. J. Comput. Vis., 92 (2011), pp. 265–280.
- [51] X.-C. TAI AND J. XU, *Global and uniform convergence of subspace correction methods for some convex optimization problems*, Math. Comp., 71 (2002), pp. 105–124.
- [52] Y. YAO, G. LI, AND P. QIN, *Seepage features of high-velocity non-Darcy flow in highly productive reservoirs*, J. Nat. Gas Sci. Eng., 27 (2015), pp. 1732–1738.
- [53] X. ZHANG, *Multilevel Schwarz methods*, Numer. Math., 63 (1992), pp. 521–539.
- [54] X. ZHANG, *Multilevel Schwarz methods for the biharmonic Dirichlet problem*, SIAM J. Sci. Comput., 15 (1994), pp. 621–644.
- [55] I. ZIÓŁKOWSKA AND D. ZIÓŁKOWSKI, *Fluid flow inside packed beds*, Chem. Eng. Process., 23 (1988), pp. 137–164.